

Synthesis, structures, and alkene hydrosilation activities of neutral tripodal amidozirconium alkyls

Li Jia,^{a*} Jiquan Zhao,^a Errun Ding^a and William W. Brennessel^b

^a Department of Chemistry, Lehigh University, Bethlehem, PA 18015, USA.

E-mail: lij4@lehigh.edu

^b Department of Chemistry, University of Minnesota, Minneapolis, MN 55455, USA

Received 22nd January 2002, Accepted 2nd May 2002

First published as an Advance Article on the web 29th May 2002

Aminolysis of $\text{Zr}(\text{CH}_2\text{C}_6\text{H}_5)_4$ with $\text{CH}[(\text{CH}_3)_2\text{SiNHAr}]_3$ (Ar = *para*-tolyl and *para*-fluorophenyl) affords $\text{CH}[(\text{CH}_3)_2\text{SiNAr}]_3\text{ZrCH}_2\text{C}_6\text{H}_5$ **1a** and **1b** (a: Ar = *para*-tolyl; b: Ar = *para*-fluorophenyl). Solution and solid state X-ray structural data suggest an η^2 -bonding mode for the benzyl group in **1a** and **1b**. Treating **1a** and **1b** with *N,N*-dimethylanilinium chloride or triphenylmethyl chloride yields $\text{CH}[(\text{CH}_3)_2\text{SiNAr}]_3\text{ZrCl}$ (**2a** and **2b**). Complex **2a** exhibits a fast dimer–monomer equilibrium in benzene. Single-crystal X-ray diffraction of **2a** reveals a dimeric structure bridged by two μ -Cl atoms. Metathesis of **2a** and **2b** with *n*-butyllithium in toluene and then in hexane yields $\text{CH}[(\text{CH}_3)_2\text{SiNAr}]_3\text{Zr}^n\text{Bu}$ (**3a** and **3b**). The crystal structures and the IR spectra of **3a** and **3b** in Nujol mulls reveal weak β -agostic interactions, but solution NMR spectra of **3a** and **3b** give no evidence for such a motif. Further, the larger Zr–C α –C β angles and the longer Zr–C β distances suggest the β -agostic interactions in **3a** and **3b** are weaker than those in the previously reported cases of Group 4 metals. Complexes **1a**, **1b**, **3a**, and **3b** are active alkene hydrosilation catalysts. The catalytic activities exhibited by these complexes are in contrast to the inertness of the previously reported neutral molecules of the type X_3MR (X = amide, alkoxide, or siloxide; M = Group 4 metal; R = alkyl or hydride). We attribute the improved activity to three factors: the small ancillary groups of the ligand, the accessibility of the coordination sites *cis* to the Zr–alkyl group due to the small “bite angle” of the ligand, and the weakened $\text{N}(\text{p}) \rightarrow \text{Zr}(\text{d}) \pi$ donation due to the coordination geometry imposed by the tripodal ligand.

Introduction

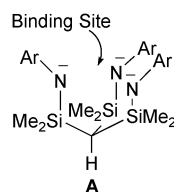
High electrophilicity is a necessary condition for Group 4 d^0 organometallic complexes to exhibit catalytic activities based on alkene insertion and σ -bond metathesis. The vast majority of recent research in this area has subsequently focused on complexes with a net positive charge.^{1,2} However, Jordan, Bercaw, and Bochmann have demonstrated that neutral zirconium molecules isoelectronic to the cationic metallocene complexes are also active catalysts for ethylene polymerization and alkyne hydrogenation although their activities are generally one to two magnitudes lower than those of the cationic complexes.^{3,4} It seems logical to expect that high electrophilicity can also be achieved using electron-withdrawing ligands such as alkoxides and amides and yet molecules with the general formula X_3MR (X = alkoxide, siloxide, or amide; M = Group 4 metal; R = alkyl or H) are very inert.⁵ Although most X_3MR molecules contain voluminous X ligands, the benzyltitanium silsesquioxide reported by Duchateau *et al.* is sterically rather open but still lacks the Lewis acidity to form adducts with acetonitrile,^{5a} suggesting that the low reactivity cannot be ascribed solely to the steric bulkiness of the ligand X. On the other hand, the tetra-coordinate species $(\text{SiO})_3\text{ZrH}$ generated by supporting ZrR_4 complexes on a partially dehydrated silica surface is believed to be the active component for hydrogenolysis of polyethylene and polymerization of ethylene.⁶ The striking reactivity differences between the soluble molecules and the putative surface-immobilized species are thus puzzling.

A general structural feature of X_3MR molecules, including the halides (R = halide), is that the X–M–X angles exceed the ideal tetrahedral angle of 109.5° (the average of the three X–M–X angles reported in the literature range from 111 to 116°).^{5,7} The steric encumbrance of the X ligands is usually cited as the reason for the large angles. If so, the average N–

M–N angles in the $(\text{TMS}_2\text{N})_3\text{MCl}$ series (M = Ti, Zr, and Hf) should follow the order $\text{N–Ti–N} > \text{N–Zr–N} \approx \text{N–Hf–N}$, because the ionic radius of Ti is the smallest and should cause the strongest steric repulsion of the TMS_2N -ligands. This is actually not observed ($\text{N–Ti–N} = 114.3(3)^\circ$, $\text{N–Zr–N} = 114.1(1)^\circ$, and $\text{N–Hf–N} = 115.4(2)^\circ$). Adding to the comparison, the average N–Th–N angle in $(\text{TMS}_2\text{N})_3\text{Th}(\mu\text{-BH}_4)$ is $115.9(2)^\circ$.^{7a} It appears, at least in some cases, not completely satisfactory to explain the large angles only on a steric basis. We suspect that the large-angle coordination geometries were adopted in part because it facilitated the $\text{X}(\text{p}) \rightarrow \text{M}(\text{d}) \pi$ interaction (see discussions on structure–reactivity relationships below), which is believed to exist in the bonding between the Group 4 metals and the X ligands.⁷ The π donation decreases the electrophilicity and consequently the reactivity of the metal. The X_3MR complexes with small X–M–X angles are thus very interesting for us.

In a series of elegant reports, Gade *et al.* has systematically investigated the synthesis of Group 4 metal complexes with tripodal amide ligands and their reactivities with organic carbonyl compounds.⁸ The small N–M–N angle forced by the tripodal ligand framework was a general structural feature of Gade’s complexes. For the aforementioned reasons, we believe that this feature warrants investigations on the alkene insertion and σ -bond metathesis of these types of complexes. Among the tripodal frameworks reported by Gade, type **A** has a small binding site that appears slightly mismatched with the relatively large zirconium ion.^{8g} This property is particularly attractive to us for generating Zr–alkyl species with the smallest possible N–Zr–N angles.

We have communicated that the hydrido and benzylzirconium complexes supported by the ligand **A** with Ar = *para*-tolyl undergo ethylene multiple insertions and produce polyethylene at very slow rates.⁹ This reactivity was not previously observed

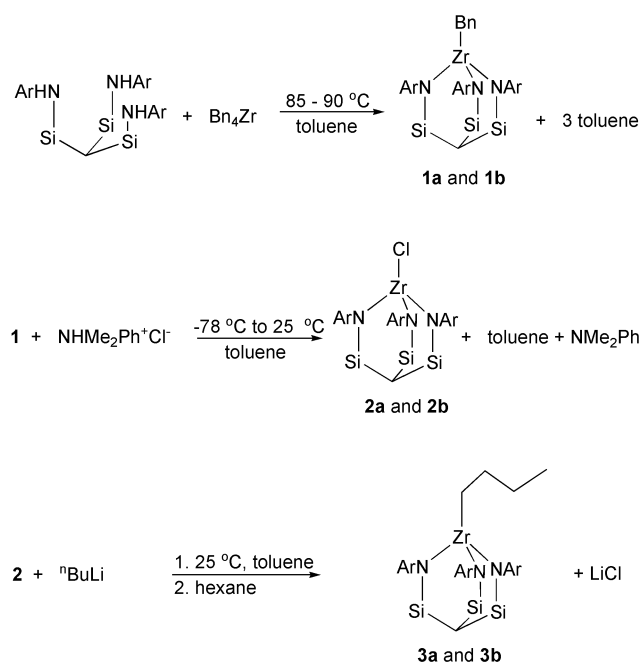


for X_3MR complexes. We report here a full account of the synthesis, characterization, and catalytic alkene-hydrosilation activities of the zirconium complexes supported by the ligand type **A** having peripheral substituents with varied electronic characters (Ar = *para*-tolyl and *para*-fluorophenyl). The β -agostic structures observed in some of the alkyl complexes indicate a relatively high level of electronic unsaturation of the zirconium in these complexes. The catalytic hydrosilation activity is unprecedented for the X_3MR complexes. In addition to the steric effects of the tripodal ligands on the reactivity, we will also discuss the possible electronic effects caused by the orbital interactions between zirconium and the tripodal ligands.

Results and discussion

Synthesis of benzyl complexes (**1a** and **1b**)

The benzyl complexes **1a** and **1b** proved to be valuable starting materials for the synthesis of zirconium complexes supported by the specific tripodal amide ligands. They are obtained in a straightforward manner by aminolysis of tetrabenzylzirconium using the amine precursors of the corresponding ligands (Scheme 1). The preparation of **1a** reaches completion in 1 day



Scheme 1 Synthesis of tripodal amidozirconium complexes. **a**: Ar = *para*-tolyl; **b**: Ar = *para*-fluorophenyl. Methyl groups attached to Si atoms in the ligand framework are omitted for clarity.

at 60 °C and is essentially quantitative by NMR, while the preparation of **1b** requires 85 °C and takes 3 days. The temperature is crucial for the preparation of **1b**. Reactions at temperatures above 90 °C result in mixtures that contain **1b** but are difficult to purify.

Both **1a** and **1b** are in time-average C_{3v} symmetry on the NMR time scale at room temperature in benzene- d_6 solution. The same symmetry property is observed for all complexes that will be reported in the following text and will not be reiterated. The benzyl groups in both **1a** and **1b** are bonded to zirconium in the η^2 mode in benzene- d_6 solution, as evidenced by the high-

field chemical shifts of the *ortho* protons of the benzyl groups (δ 6.04 and 5.95 ppm for **1a** and **1b**, respectively) and the large 1H - ^{13}C coupling constants of the methylene unit ($^1J_{H-C}$ = 129 and 131 Hz for **1a** and **1b**, respectively).¹⁰ The coupling constants suggest that the phenyl-Zr interaction is slightly stronger in **1b** than in **1a**.

The solid state structure of **1b** was determined by X-ray diffraction (Fig. 1). Complex **1b** is isostructural to **1a**, the structure

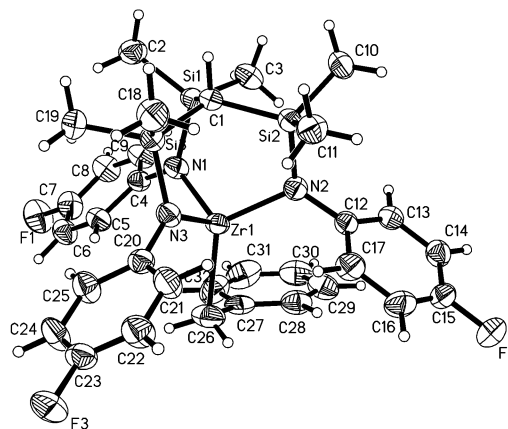


Fig. 1 ORTEP²⁴ drawing of **1b**. Thermal ellipsoids shown at 50% probability.

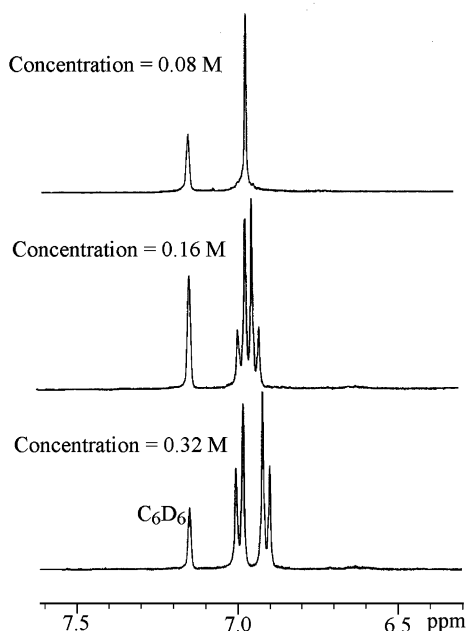
of which was communicated earlier.⁹ Selected interatomic distances and angles for **1b** are listed in Table 1. The benzyl group in **1b** is η^2 -bonded to zirconium in the solid state the same as in **1a**. The Zr-CH₂-C_{ipso} angle in **1b** (88.24(14)°) is smaller than those in **1a** (91.4(5) and 93.1(5)° in two crystallographically independent molecules), and the Zr-C_{ipso} contact in **1b** (2.648(2) Å) is shorter than those in **1a** (2.753(7) and 2.795(8) Å in the two crystallographically independent molecules).⁹ Thus, both the solid state X-ray data and the solution data suggest a stronger phenyl-Zr interaction in **1b** than in **1a**. This difference can apparently be explained by the electron-withdrawing ability of the fluorinated ligand resulting in an increase in zirconium electrophilicity. The Zr-N distances are unexceptional, and the nitrogen atoms of the arylamide are nearly planar as in all early transition metal amide compounds. The planes that contain the zirconium arylamides twist away slightly from the pseudo- C_3 axis that passes C(1) and Zr(1) by 7 to 22°.

Synthesis of chloride complexes **2a** and **2b**

Gade recently reported the synthesis of the etherate and the LiCl adduct of **2a** by reaction of ZrCl₄ with the lithium salt of the corresponding ligand.^{8c} Lewis base-free chloride complexes with tripodal amide ligands bulkier and more electron-donating than the ones used here were synthesized using the same metathesis approach.^{8a} We found that Lewis base-free **2a** and **2b** can be obtained by reaction of **1a** and **1b**, respectively, with a proton source or an alkyl abstractor (Scheme 1). The reactions are quantitative, and the isolated yields are good. Attempts to determine whether **2a** and **2b** exist as dimers or monomers in benzene solution by freezing point depression were unsuccessful due to the insufficient solubility of the two compounds. Interestingly, the 1H NMR spectrum of **2a** is dependent on the concentration. The change is reversible and most noticeably occurs in the aromatic region (Fig. 2). Our explanation of the concentration dependence is that the 1H NMR spectra are the average spectra of a fast equilibrium between the monomer and the dimer of **2a**. The spectrum at high concentrations displaying two doublets of AX spins essentially belongs to the dimer. The spectrum at low concentrations displaying a singlet of A2 spins belongs to the monomer. At intermediate concentrations, the differences between the average chemical shifts of the A2 and AX spins are comparable to the coupling constant

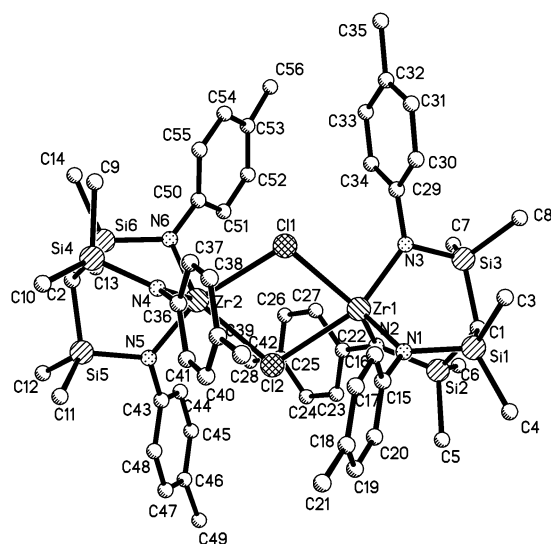
Table 1 Selected interatomic distances (Å), angles (°), and torsion angles (°) in **1b**

Zr(1)–C(26)	2.246(2)	Zr(1)–N(2)	2.0680(17)
Zr(1)–C(27)	2.648(2)	Zr(1)–N(3)	2.0644(17)
Zr(1)–N(1)	2.0773(18)		
C(27)–C(26)–Zr(1)	88.24(14)	N(1)–Zr(1)–N(3)	99.92(7)
N(1)–Zr(1)–N(2)	108.86(7)	N(2)–Zr(1)–N(3)	101.08(7)
C(4)–N(1)–Zr(1)–C(1)	158.07(19)	C(20)–N(3)–Zr(1)–C(1)	173.5(2)
C(12)–N(2)–Zr(1)–C(1)	163.59(17)		

**Fig. 2** Concentration-dependent ^1H NMR spectra of **2a** (360 MHz, 25 °C, benzene- d_6).

($J = 7.3$ Hz), resulting in the second-order spectra of AB spins. No change of the ^1H NMR spectrum of **2b** can be detected at various concentrations.

The crystal structure of **2a** shows that it is a dimer bridged by two $\mu\text{-Cl}$ atoms in the solid state (Fig. 3). The selected geometric parameters are listed in Table 2. The Si and N atoms on one side of the dimer are positionally disordered and refined at the 77 : 23 ratio of occupancy. The opposite side also shows a similar disorder but to such a small extent as to be negligible. The

**Fig. 3** Molecular structure of **2a**. Hydrogen atoms are omitted for clarity.

Zr–N distances in the minor component of the disorder are in parentheses (Table 2). The geometry of the tripodal ligands around the two metal centers is very similar to that of **1b** described above. The X-ray diffraction data of **2b** suffered from loss of co-crystallized solvent molecules, but were sufficient to show the dimeric nature of **2b** with two Cl bridges in the solid state.

Synthesis of *n*-butyl complexes **3a** and **3b**

Gade recently reported that Lewis base-free methyl complexes with tripodal amide ligands bulkier and more electron-donating than the ones used here could be synthesized by reaction of the corresponding chloride complexes with LiMe or MgBrMe.^{8a} However, reactions of **2a** with LiMe or MgBrMe inevitably form the methylzirconium etherates. Our attempts to use Me₃Al and Et₂Zn as the alkylating reagents for the synthesis of Lewis base-free alkylzirconium complexes also proved unsuccessful. On the other hand, synthesis of the Lewis base-free butyl complexes **3a** and **3b** is successful using *n*-butyllithium (Scheme 1). The reactions are carried out in toluene, but precipitation of LiCl is not obvious presumably because LiCl remains coordinated with zirconium. Stirring the mixtures in hexane extracts the product and leaves LiCl in the solid. The ^1H NMR spectra of **3a** and **3b** in benzene- d_6 solution provide no evidence for agostic interactions between the butyl and zirconium, showing normal chemical shifts and coupling constants ($^1J_{\text{Ca-H}} = 114$ and $^1J_{\text{C}\beta\text{-H}} = 120$ Hz for **3a**, $^1J_{\text{Ca-H}} = 116$ and $^1J_{\text{C}\beta\text{-H}} = 120$ Hz for **3b**).^{11–14}

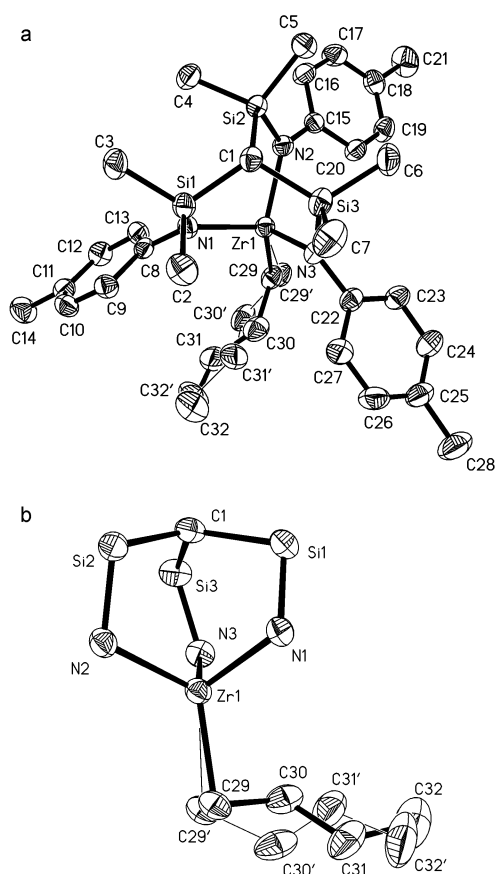
The crystal structures of **3a** and **3b** were determined by X-ray diffraction (Figs. 4 and 5). Selected interatomic distances and bond angles are listed in Tables 3 and 4. As generally observed for the tripodal amide complexes,^{8,9} the N–Zr–N angles are very small, and the Zr–N distances are unexceptional. Some interesting features exist concerning the bonding between the butyl and the zirconium. The structure of **3b** contains a butyl group that appears involved in a weak interaction with zirconium at the β -position. The $\text{C}\beta\text{--Ca--Zr}$ angle of $95.7(10)^\circ$ is much larger than the $\text{C}\beta\text{--Ca--M}$ angles previously observed for β -agostic Group 4 metal alkyls ($86.3(6)^\circ$ in $(\text{DMPE})\text{Cl}_3\text{TiEt}$ and $84.7(5)^\circ$ in $\text{Cp}_2\text{ZrEt}(\text{PMe}_3)^+$),^{12,14} but is much smaller than the $\text{C}\beta\text{--Ca--M}$ angle in non-agostic structures, where the angle is typically in the range from 108 to 126° .^{11,12} The $\text{C}\beta\text{--Zr}$ distance of $2.798(5)$ Å is long compared to that in $\text{Cp}_2\text{ZrEt}(\text{PMe}_3)^+$ ($2.629(9)$ Å). The short Ca--Zr distance of $2.19(2)$ Å is common for tetracoordinate zirconium alkyl complexes,^{5d} although the contribution from the β -agostic interaction can not be ruled out. The butyl group in **3a** is disordered and satisfactorily modeled over two positions at a 50 : 50 occupancy ratio. The two positions represent the coexistence of a weakly β -agostic butyl and a non-agostic butyl. The $\text{C}\beta\text{--Ca--Zr}$ angle and the $\text{C}\beta\text{--Zr}$ distance of the agostic Zr-butyl group of **3a** are similar to those in **3b** (Table 4). IR spectra in Nujol mulls of both complexes exhibit weak low-frequency $\nu(\text{C--H})$ bands (2571 , 2500 , and 2466 cm^{-1} for **3a**, and 2574 , 2504 , and 2443 cm^{-1} for **3b**), indicative of weakened C–H bonds.^{11–13} Thus, in the continuum of β -agostic interaction, the solid state structures of **3a** and **3b** serve as examples of very weak interactions, which seems to recede in solution.

Table 2 Selected interatomic distances (Å), angles (°), and torsion angles (°) in **2a**

Zr(1)–Cl(1)	2.5761(8)	Zr(1)–N(2)	2.081(4) (1.951(14))
Zr(1)–Cl(2)	2.6385(8)	Zr(1)–N(3)	2.064(4) (2.082(14))
Zr(2)–Cl(1)	2.6428(8)	Zr(2)–N(4)	2.033(2)
Zr(2)–Cl(2)	2.5660(8)	Zr(2)–N(5)	2.048(2)
Zr(1)–N(1)	2.020(5) (2.030(18))	Zr(2)–N(6)	2.076(2)
N(1)–Zr(1)–N(2)	100.59(13) (100.5(5))	N(4)–Zr(2)–N(5)	98.20(9)
N(1)–Zr(1)–N(3)	100.39(15) (96.0(6))	N(4)–Zr(2)–N(6)	100.94(10)
N(2)–Zr(1)–N(3)	98.14(13) (96.9(5))	N(5)–Zr(2)–N(6)	99.07(9)
C(15)–N(1)–Zr(1)–C(1)	171.6(5)	C(36)–N(4)–Zr(2)–C(2)	161.2(3)
C(22)–N(2)–Zr(1)–C(1)	162.4(4)	C(43)–N(5)–Zr(2)–C(2)	164.1(3)
C(29)–N(3)–Zr(1)–C(1)	173.7(4)	C(50)–N(6)–Zr(2)–C(2)	171.2(3)

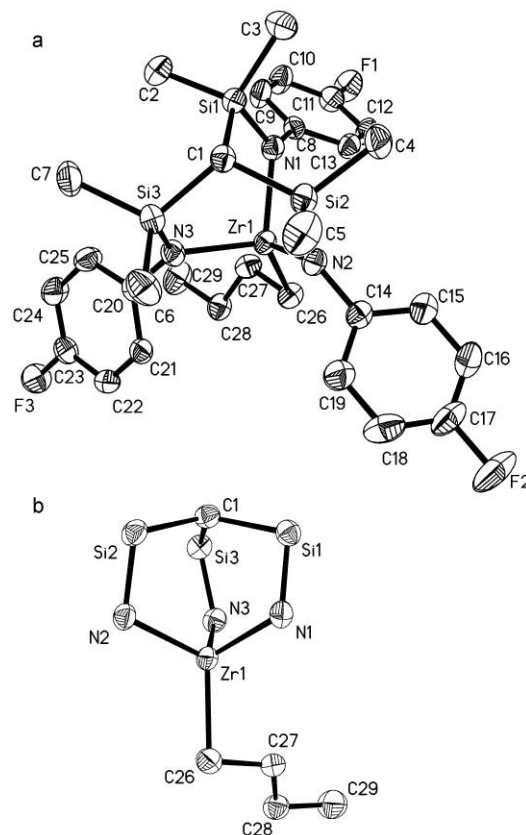
Table 3 Selected interatomic distances (Å), angles (°), and torsion angles (°) in **3a**

Zr(1)–C(29)	2.19(2)	Zr(1)–N(2)	2.0751(16)
Zr(1)–C(30)	2.798(5)	Zr(1)–N(3)	2.0452(17)
Zr(1)–C(29')	2.27(2)	C(29)–C(30)	1.542(9)
Zr(1)–C(30')	3.252(5)	C(29')–C(30')	1.538(9)
Zr(1)–N(1)	2.0706(16)		
C(30)–C(29)–Zr(1)	95.7(10)	N(2)–Zr(1)–C(29')	117.7(3)
C(30')–C(29')–Zr(1)	115.9(11)	N(3)–Zr(1)–C(29')	110.3(4)
N(1)–Zr(1)–C(29)	114.2(4)	N(1)–Zr(1)–N(2)	102.09(6)
N(2)–Zr(1)–C(29)	122.5(3)	N(1)–Zr(1)–N(3)	102.48(7)
N(3)–Zr(1)–C(29)	112.3(5)	N(2)–Zr(1)–N(3)	100.75(7)
N(1)–Zr(1)–C(29')	120.8(4)		
C(8)–N(1)–Zr(1)–C(1)	171.49(16)	C(22)–N(3)–Zr(1)–C(1)	175.07(18)
C(15)–N(2)–Zr(1)–C(1)	158.89(17)		

**Fig. 4** ORTEP drawings of **3a**. Thermal ellipsoids shown at 50% probability. (a) Top view. Hydrogen atoms are omitted for clarity. (b) Side view with peripheral groups omitted.

Catalytic alkene hydrosilation

Compounds **1a**, **1b**, **3a**, and **3b** can be used as catalyst precursors for 1-hexene hydrosilation (Table 5). All the pre-

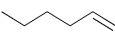
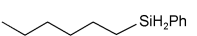


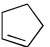
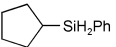
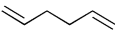
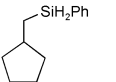
**Fig. 5** ORTEP drawings of **3b**. Thermal ellipsoids shown at 50% probability. (a) Top view. Hydrogen atoms are omitted for clarity. (b) Side view with peripheral groups omitted.

catalysts are very stable for several days in toluene at a 90 °C reaction temperature. The catalytic reactions are highly selective and practically quantitative in all experiments. Methylene cyclopentane is accumulated during the course of hydrosilation of 1,5-hexadiene and is eventually hydrosilated (entries 7 and 8, Table 5). For catalysts **1a** and **1b**, initial

Table 4 Selected interatomic distances (Å), bond angles (°), and torsion angles (°) in **3b**

Zr(1)–C(26)	2.209(2)	Zr(1)–N(2)	2.0540(18)
Zr(1)–C(27)	2.842(2)	Zr(1)–N(3)	2.0660(18)
Zr(1)–N(1)	2.0684(18)	C(26)–C(27)	1.535(3)
C(27)–C(26)–Zr(1)	97.12(14)	N(1)–Zr(1)–N(2)	104.05(7)
N(1)–Zr(1)–C(26)	116.12(8)	N(1)–Zr(1)–N(3)	102.56(7)
N(2)–Zr(1)–C(26)	114.76(8)	N(2)–Zr(1)–N(3)	102.14(7)
N(3)–Zr(1)–C(26)	115.36(7)		
C(8)–N(1)–Zr(1)–C(1)	179.91(17)	C(20)–N(3)–Zr(1)–C(1)	172.75(19)
C(14)–N(2)–Zr(1)–C(1)	170.9(2)		

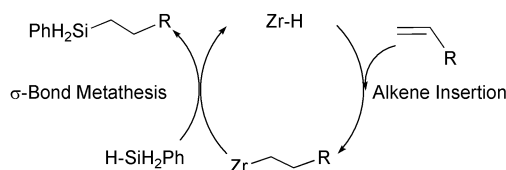
Table 5 Catalytic olefin hydrosilation^a

Entry	Alkene	Catalyst (2 mol%)	Reaction half-life ^b /h	Reaction time/h	Product	Isolated yield (%)
1		1a	—	187		87
2		1b	—	134		94
3		3a	6	69		90
4		3b	4	50		92
5		3a	20	340		90
6		3b	11	297		90
7		3a	18	183		89
8		3b	9	110		91

^a Reaction carried out at 90 °C in neat alkene. ^b Based on silane consumption estimated by ¹H NMR integration.

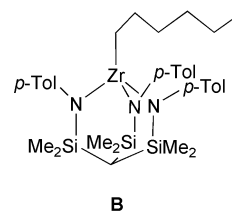
cleavage of the benzyl group is very slow compared to the subsequent turnovers of the catalytic process, for example, at the completion of hydrosilation of 1-hexene, 37% of **1a** and 66% of **1b** remain unconverted to the active species (entries 1 and 2, Table 5). Initiation of the catalytic process is fast for the butyl complexes **3a** and **3b**, allowing direct comparison of their catalytic activities. Catalyst **3b** is always more efficient than **3a** (entries 3 vs. 4, 5 vs. 6, and 7 vs. 8, Table 5). The half-lives of phenylsilane in reactions catalyzed by **3b** are generally one half to two thirds of those in the corresponding reactions catalyzed by **3a**. The activities of **3a** and **3b**, however, are several magnitudes lower than those of the lanthanide and yttrium hydrosilation catalysts.¹⁵

With regard to the mechanism of the hydrosilation, it is unlikely that any low-valent zirconium species are involved as in the Cp₂ZrCl₂/BuLi systems.¹⁶ We propose that the mechanism is similar to that of the lanthanide and yttrium-catalyzed hydrosilation comprising of alkene insertion into the metal–H bond and σ-bond metathesis between the H–Si bond and the metal–alkyl bond (Scheme 2).¹⁵

**Scheme 2** Proposed hydrosilation mechanism.

The structural integrity of the tripodal framework and thus the mechanism are supported by the following experiment. In a **3a**-catalyzed 1-hexene hydrosilation experiment, 1-hexene in two-fold excess to phenylsilane was used. After the silane was completely consumed, the volatile component of the reaction

mixture was removed under high vacuum at 60 °C. ¹H and ¹³C NMR clearly showed that the hexyl derivative, **B**, was the only component in the pale yellow semi-solid residue. Note that **B** can be independently synthesized through 1-hexene insertion into the isolated zirconium hydride complex.⁹



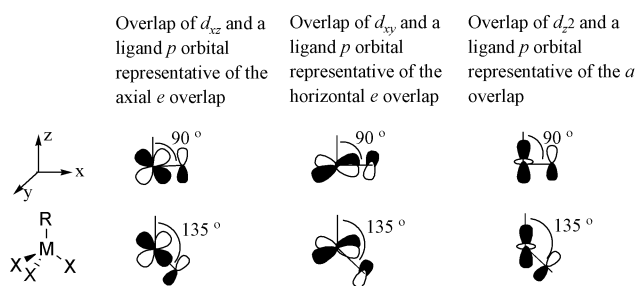
Structure–reactivity relationship of the X₃MR complexes

The catalytic activities of alkene hydrosilation and ethylene polymerization that we have communicated,⁹ albeit low, have never been observed for the X₃MR complexes (X = amide, alkoxide, or siloxide; R = alkyl or H).^{5a} It is interesting to question why the differences in reactivity are present.

Sterically, voluminous amide or alkoxide ligands are usually employed to stabilize X₃MR complexes when X is a monodentate anionic ligand in order to suppress the ligand redistribution tendency of the electropositive metals. Gade's tripodal ligands allow significant reduction of the overall steric hindrance around the metal without compromising the stability with respect to ligand redistribution. The complexes discussed here show no signs of decomposition after several days at 90 °C in toluene-d₈ solution as assessed by ¹H NMR. In addition to the reduction of the size, the small binding site of the tripodal ligands also makes the zirconium easily accessible by forcing it out of the N–N–N plane (average N–Zr–N angle = 101° in **1a**, 103° in **1b**, 101.8° in **3a**, and 102.9° in **3b**). The small size and

small binding site of the tripodal ligands undoubtedly sterically opens up the coordination sites *cis* to the Zr–alkyl bond and favor the pre-coordination of reaction substrates such as alkenes and silanes.

In addition to the steric effects, the small N–Zr–N angles are possibly advantageous for enhancing the reactivity from the viewpoint of the N(p) → Zr(d) π donation. In general, the X(p) → M(d) π interactions affect the electronic properties on two fronts, the energy of the individual orbitals of d character and the overall electron density at the metal center. We will first discuss the energy of the individual d orbitals. The coordination of a substrate *cis* to the M–R bond in C_{3v} symmetry requires low-lying metal-centered e orbitals (essentially d_{xy} , $d_{x^2-y^2}$, d_{yz} , and d_{xz} orbitals) (Scheme 3).



Scheme 3 Change of π -interactions between metal-d and ligand-p orbitals.

The e combinations of the ligand p orbitals would best overlap with the d_{xy} , $d_{x^2-y^2}$, d_{yz} , and d_{xz} orbitals if the X–M bonds were perpendicular to the z-axis (trigonal pyramidal geometry with X–M–X angles being 120°). When the angles between the M–X bonds and the z-axis increase (*i.e.*, the X–M–X angles decrease), the magnitude of the e overlaps decreases (Scheme 3). The e overlap in the axial direction involving d_{yz} and d_{xz} orbitals would be completely non-bonding if the angle were 135° (Scheme 3). Consequently, the metal-centered e orbitals will be stabilized when the X–M–X angles are small. The opposite is true for the a overlap with the d_{z^2} orbital (Scheme 3). The e orbitals are required for substrate *cis* coordination, while the a orbital is insignificant for substrate coordination since its access is blocked by the collinear M–R bond.

We now consider the overall electron density at the metal center, which is affected by the total amount of π donation from the ligand p orbitals to the metal d orbitals. Since the average angles between the z-axis and the planes of the amides range from 165 – 174° in the crystal structures of **1a**, **1b**, **3a**, and **3b**, the horizontal e overlaps are fuller than the axial e and a overlaps in these cases. When the diminution of the two sets of e overlaps and the enhancement of the weak axial a interaction are both considered, the geometry with small N–Zr–N angles should cause a net decrease of overall electron density at the zirconium center compared to the geometry with large N–Zr–N angles. To summarize the above discussion, the small N–Zr–N angles are beneficial for both the stabilization of the empty d orbitals *cis* to the Zr–alkyl group (e orbitals) and the overall decrease of electron density at the metal center. The geometry-induced orbital effects are in fact reminiscent of the *ansa*-effects in the bent metallocene systems discussed by Parkin *et al.*¹⁷

Summary

We have described the synthesis, characterization, and reactivities of a group of Zr–alkyl complexes. They possess catalytic activities unprecedented for the X_3MR type complexes, but are much less reactive than the more electropositive lanthanide complexes and the Group 4 complexes with a formal cationic charge. It appears that in addition to the inductive electronic and steric effects, coordination geometry-caused orbital effects are important factors to be considered for future design of

catalytically active complexes, especially for complexes not in a bent-metallocene framework.

Experimental

All experiments were conducted using standard Schlenk line and high-vacuum (10^{-5} Torr) line techniques or in a glove box filled with nitrogen. Hydrocarbon solvents were distilled from Na/benzophenone under nitrogen and stored *in vacuo* over Na/K alloy in flasks sealed by Teflon valves. Hexamethyldisiloxane and benzene- d_6 were dried over Na/K alloy, freeze–pump–thaw degassed, and kept over Na/K alloy. $CDCl_3$ was dried by refluxing over CaH_2 , distilled, and kept over CaH_2 . Triphenylmethyl chloride was purchased from Aldrich and purified by sublimation. *N,N*-Dimethylanilinium chloride was prepared by mixing an equal molar amount of *N,N*-dimethylaniline and HCl (1.0 M in diethyl ether) in diethyl ether followed by repetitive washing with diethyl ether. Both *N,N*-dimethylaniline and the ether solution of HCl were purchased from Aldrich and used directly. Tripodal ligands $CH[(CH_3)_2SiNH(p\text{-}tolyl)]_3$,^{8f} $CH[(CH_3)_2SiNH(4\text{-}FC_6H_4)]_3$ ^{8f} and $Zr(CH_2C_6H_5)_4$ ¹⁸ were prepared using literature methods.

Synthesis

Synthesis of $CH[(CH_3)_2SiN(p\text{-}CH_3C_6H_4)]_3ZrCH_2C_6H_5$ (1a). $Zr(CH_2C_6H_5)_4$ (114 mg, 0.25 mmol) and $CH[(CH_3)_2SiNH(p\text{-}tolyl)]_3$ (127 mg, 0.25 mmol) were loaded into a 50 mL reaction flask in the glove box and dissolved in toluene (20 mL). The toluene solution was stirred and heated at $60^\circ C$ for 24 hours in the dark. Removal of the solvent *in vacuo* resulted in an off-white powder. Extraction of the solid with hexane (≈ 15 mL) and filtration yielded a pale yellow solution. Cooling the solution at $-40^\circ C$ yielded pale yellow crystals of **2** (154 mg, 90%). Anal. calc. for $C_{35}H_{47}N_3Si_3Zr$: C, 61.35; H, 6.91; N, 6.13. Found: C, 61.20; H, 6.42; N, 6.02%. 1H NMR ($20^\circ C$, C_6D_6): δ -0.50 (s, 1H, $CH\equiv$), 0.36 (s, 18H, $[(CH_3)_2Si-]_3$), 2.13 (s, 2H, $ZrCH_2C_6H_5$), 2.16 (s, 9H, $[p\text{-}C_6H_4CH_3]_3$), 6.04 (d, $J = 7.2$ Hz, 2H, *ortho* $ZrCH_2C_6H_5$), 6.59 (“t”, $J = 7.4$ Hz, 2H, *meta* $ZrCH_2C_6H_5$), 6.70 (t, $J = 7.5$ Hz, 1H, *para* $ZrCH_2C_6H_5$), 6.96 (d, $J = 7.2$ Hz, 6H, $[p\text{-}C_6H_4CH_3]_3$), 7.01 (d, $J = 7.2$ Hz, 6H, $[p\text{-}C_6H_4CH_3]_3$). $^{13}C\{^1H\}$ NMR ($20^\circ C$, C_6D_6): δ 4.1 ($[(CH_3)_2Si-]_3$), 4.2 ($HC\equiv$), 20.8 ($[p\text{-}C_6H_4CH_3]_3$), 73.3 ($ZrCH_2C_6H_5$), 123.3 (*para* $ZrCH_2C_6H_5$), 125.4 (*ortho* or *meta* $[p\text{-}C_6H_4CH_3]_3$), 126.5 (*ortho* or *meta* $ZrCH_2C_6H_5$), 130.2 (*ortho* or *meta* $ZrCH_2C_6H_5$), 130.5 (*ortho* or *meta* $[p\text{-}C_6H_4CH_3]_3$), 131.9 (*para* or *ipso* $[p\text{-}C_6H_4CH_3]_3$), 139.7 (*ipso* $ZrCH_2C_6H_5$), 146.5 (*para* or *ipso* $[p\text{-}C_6H_4CH_3]_3$).

Synthesis of $CH[(CH_3)_2SiN(p\text{-}FC_6H_4)]_3ZrCH_2C_6H_5$ (1b). Compound **1b** was synthesized following a procedure similar to that for **1a** using $Zr(CH_2C_6H_5)_4$ (228 mg, 0.500 mmol) and $CH[(CH_3)_2SiNH(p\text{-}FC_6H_4)]_3$ (259 mg, 0.50 mmol). The reaction required 3 days at $85^\circ C$. After removal of toluene, the black residue was extracted with hexamethyldisiloxane (≈ 15 mL) at $80^\circ C$. Quick filtration resulted in a yellow solution. Cooling the solution slowly to $-40^\circ C$ and keeping it overnight at such a temperature yielded pale yellow crystals of **2** (210 mg, 60%). Anal. calc. for $C_{32}H_{38}F_3N_3Si_3Zr$: C, 55.13; H, 5.49; N, 6.03. Found: C, 54.93; H, 5.42; N, 6.91%. 1H NMR ($20^\circ C$, C_6D_6): δ -0.58 (s, 1H, $CH\equiv$), 0.24 (s, 18H, $[(CH_3)_2Si-]_3$), 1.95 (s, 2H, $ZrCH_2C_6H_5$), 5.95 (d, $J = 7.2$ Hz, 2H, *ortho* $ZrCH_2C_6H_5$), 6.49 (“t”, $J = 7.4$ Hz, 2H, *meta* $ZrCH_2C_6H_5$), 6.62 (t, $J = 7.2$ Hz, 1H, *para* $ZrCH_2C_6H_5$), 6.68 – 6.86 (m, 12H, $[p\text{-}C_6H_4F]_3$). $^{13}C\{^1H\}$ NMR ($20^\circ C$, C_6D_6): δ 3.2 ($HC\equiv$), 4.2 ($[(CH_3)_2Si-]_3$), 73.9 ($ZrCH_2C_6H_5$), 116.3 (d, $^2J_{C-F} = 21$ Hz, *meta* $[p\text{-}C_6H_4F]_3$), 124.2 (*para* $ZrCH_2C_6H_5$), 126.3 (overlap of *ortho* $[p\text{-}C_6H_4F]_3$ and *ortho* or *meta* $ZrCH_2C_6H_5$), 130.8 (*ortho* or *meta* $ZrCH_2C_6H_5$), 138.4 (*ipso* $ZrCH_2C_6H_5$), 145.6 (*ipso* $[p\text{-}C_6H_4F]_3$), 159.4 ($^1J_{C-F} = 239$ Hz, *para* $[p\text{-}C_6H_4F]_3$).

Table 6 Crystal data and structure refinements for **1b**, **2a**, **3a**, and **3b**

	1b	2a	3a	3b
Empirical formula	C ₃₂ H ₃₈ F ₃ N ₃ Si ₃ Zr	C ₅₆ H ₈₀ Cl ₂ N ₆ Si ₆ Zr ₂	C ₃₂ H ₄₀ N ₃ Si ₃ Zr	C ₂₉ H ₄₀ F ₃ N ₃ Si ₃ Zr
Formula weight	697.14	1259.14	651.23	663.13
Crystal system	Orthorhombic	Monoclinic	Monoclinic	Monoclinic
Space group	<i>P</i> 2 ₁ 2 ₁ 2 ₁	<i>P</i> 2 ₁ / <i>c</i>	<i>C</i> 2/ <i>c</i>	<i>P</i> 2 ₁ / <i>n</i>
<i>a</i> /Å	11.6166(6)	13.700(3)	42.402(3)	9.576(1)
<i>b</i> /Å	14.3844(8)	25.525(5)	9.9224(7)	19.106(2)
<i>c</i> /Å	20.310(1)	18.183(4)	17.614(1)	18.087(2)
β /°	90	94.187(4)	108.717(1)	97.160(2)
Volume/Å ³	3393.7(3)	6341(2)	7018.8(8)	3283.3(6)
<i>Z</i>	4	4	8	4
Absorption coefficient/mm ^{−1}	0.472	0.566	0.440	0.484
Crystal color, habit	Colorless, block	Pale yellow, block	Pale yellow, block	Colorless, block
Crystal size/mm ³	0.29 × 0.26 × 0.26	0.29 × 0.22 × 0.19	0.28 × 0.22 × 0.19	0.26 × 0.26 × 0.25
Reflections collected	25607	37121	20413	21519
Independent reflections	5994 [<i>R</i> (int) = 0.0223]	11187 [<i>R</i> (int) = 0.0324]	6196 [<i>R</i> (int) = 0.0233]	5808 [<i>R</i> (int) = 0.0249]
Refined parameters	385	794	393	358
Goodness-of-fit on <i>F</i> ²	0.995	1.006	1.025	1.010
Final <i>R</i> indices [<i>I</i> > 2σ(<i>I</i>)]	<i>R</i> 1 = 0.0210 <i>wR</i> 2 = 0.0508	<i>R</i> 1 = 0.0362 <i>wR</i> 2 = 0.0766	<i>R</i> 1 = 0.0263 <i>wR</i> 2 = 0.0677	<i>R</i> 1 = 0.0283 <i>wR</i> 2 = 0.0766
<i>R</i> indices (all data)	<i>R</i> 1 = 0.0231 <i>wR</i> 2 = 0.0519	<i>R</i> 1 = 0.0530 <i>wR</i> 2 = 0.0824	<i>R</i> 1 = 0.0374 <i>wR</i> 2 = 0.0712	<i>R</i> 1 = 0.0377 <i>wR</i> 2 = 0.0808

Synthesis of CH[(CH₃)₂SiN(*p*-CH₃C₆H₄)]₃ZrCl (2a**).** Compound **1a** (0.684 g, 1.0 mmol) and C₆H₅NMe₂·HCl (0.142 mg, 1.00 mmol) were loaded into a 50 mL flask in the glove box. The flask was attached to the vacuum line and evacuated, and toluene (30 mL) was condensed into the flask at −78 °C. The flask was backfilled with nitrogen and warmed to room temperature slowly with stirring. After the reaction mixture was stirred for 6 h at 25 °C, toluene was removed *in vacuo*. The residue was extracted with boiling hexane (10 mL) and quickly filtered. The filtrate was allowed to stand at room temperature overnight. Pale yellow crystals were obtained (0.357 g, 56.8%). Anal. calc. for C₂₈H₄₀ClN₃Si₃Zr: C, 53.50; H, 6.39; N, 6.69. Found: C, 53.20; H, 6.45; N, 6.74%. ¹H NMR (20 °C, C₆D₆): δ −0.45 (s, 1H, HC≡), 0.32 (s, 18H, [(CH₃)₂Si−]), 2.15 (s, 9H, [*p*-C₆H₄CH₃]), 6.90 (d, *J* = 7.3 Hz, 6H, [*p*-C₆H₄CH₃]), 7.00 (d, *J* = 7.3 Hz, 6H, [*p*-C₆H₄CH₃]). ¹³C{¹H} NMR (20 °C, C₆D₆): δ 3.7 (s, HC≡), 3.9 (s, [(CH₃)₂Si−]), 20.8 ([*p*-C₆H₄CH₃]), 124.6 (*ortho* or *meta* [*p*-C₆H₄CH₃]), 130.5 (*ortho* or *meta* [*p*-C₆H₄CH₃]), 132.4 (*para* or *ipso* [*p*-C₆H₄CH₃]), 145.5 (*para* or *ipso* [*p*-C₆H₄CH₃]).

Synthesis of CH[(CH₃)₂SiN(*p*-FC₆H₄)]₃ZrCl (2b**).** Compound **2b** was synthesized following a procedure similar to that for **2a** except that **1b** (0.696 g, 1.00 mmol) and triphenylmethyl chloride (0.278 g, 1.00 mmol) were used as the starting materials. After the reaction was finished, the volume of toluene was reduced to 15 mL. The resulting slurry was heated at 100 °C and quickly filtered. The filtrate was allowed to stand overnight at room temperature. White square crystals were obtained (0.51 g, 79.7%). Anal. calc. for C₂₅H₃₁ClF₃Si₃Zr: C, 46.87; H, 4.84; N, 6.56. Found: C, 46.75; H, 4.83; N, 6.59%. ¹H NMR (20 °C, C₆D₆): δ −0.56 (s, 1H, HC≡), 0.11 (s, 18H, [(CH₃)₂Si−]), 6.56–6.57 (m, 6H *ortho* [*p*-C₆H₄F]), 6.87 (m, 6H, *meta* [*p*-C₆H₄F]). ¹³C{¹H} NMR (20 °C, CDCl₃): δ 3.8 ([[(CH₃)₂Si−]), 5.2 (s, HC≡), 115.5 (d, ²*J*_{FC} = 22 Hz, *meta* [*p*-C₆H₄F]), 125.9 (d, ³*J*_{FC} = 8 Hz, *ortho* [*p*-C₆H₄F]), 145.4 (*ipso* [*p*-C₆H₄F]), 158.8 (d, ¹*J*_{FC} = 239 Hz, *para* [*p*-C₆H₄F]).

Synthesis of CH[(CH₃)₂SiN(*p*-CH₃C₆H₄)]₃Zr⁺Bu (3a**).** Compound **2a** (0.810 g, 1.29 mmol) was loaded into a 50 mL flask in the glove box. The flask was attached to the vacuum line and evacuated. Toluene (20 mL) was condensed into the flask under vacuum at −78 °C. The flask was backfilled with nitrogen, and ⁿBuLi (0.52 mL, 2.5 M in hexane) was injected into the flask at −78 °C. The reaction mixture was warmed to room temperature slowly and was stirred for 3 h. Toluene was then removed, and hexane (5 mL) was condensed into the flask. The mixture

was stirred in hexane for 1 h at the room temperature and was filtered to remove LiCl. Hexane was then removed *in vacuo*. Next, hexamethyldisiloxane (10 mL) was condensed into the flask. Heating the mixture at 80 °C resulted in a yellow homogeneous solution. Pale yellow crystals formed overnight at room temperature (0.487 g, 58%). Anal. calc. for C₃₂H₄₉N₃Si₃Zr: C, 59.08; H, 7.54; N, 6.46. Found: C, 57.92; H, 7.60; N, 6.27%. ¹H NMR (20 °C, C₆D₆): δ −0.58 (s, 1H, HC≡), 0.45 (s, 18H, [(CH₃)₂Si−]), 0.48 (t, *J* = 7.2 Hz, 2H, ZrCH₂CH₂CH₂CH₃), 0.67 (t, *J* = 7.2 Hz, 3H, ZrCH₂CH₂CH₂CH₃), 0.75 (m, 2H, ZrCH₂CH₂CH₂CH₃), 1.04 (m, 2H, ZrCH₂CH₂CH₂CH₃), 2.11 (s, 9H, [*p*-C₆H₄CH₃]), 7.02 and 7.07 (AB spin system, *J* = 7.2 Hz, 12H, [*p*-C₆H₄CH₃]). ¹³C{¹H} NMR (20 °C, C₆D₆): δ 2.9 (HC≡), 4.2 ([[(CH₃)₂Si−]), 13.8 (ZrCH₂CH₂CH₂CH₃), 20.74 ([*p*-C₆H₄CH₃]), 27.2 (ZrCH₂CH₂CH₂CH₃), 28.52 (ZrCH₂CH₂CH₂CH₃), 70.0 (ZrCH₂CH₂CH₂CH₃), 125.0 (*ortho* or *meta* [*p*-C₆H₄CH₃]), 130.7 (*ortho* or *meta* [*p*-C₆H₄CH₃]), 131.9 (*ipso* or *para* [*p*-C₆H₄CH₃]), 144.7 (*ipso* or *para* [*p*-C₆H₄CH₃]).

Synthesis of CH[(CH₃)₂SiN(*p*-FC₆H₄)]₃Zr⁺Bu (3b**).** Compound **3b** was synthesized following a procedure similar to that for **3a** except that **2b** (0.640 g, 1.00 mmol) and ⁿBuLi (0.40 mL, 2.5 M in hexane) were used as the starting materials. The product was isolated from its hexane solution at −78 °C as colorless crystals (0.43 g, 64.9%). Anal. calc. for C₂₉H₄₀F₃N₃Si₃Zr: C, 52.57; H, 6.04; N, 6.34. Found: C, 52.47; H, 6.10; N, 6.24%. ¹H NMR (20 °C, C₆D₆): δ −0.67 (s, 1H, HC≡), 0.30 (s, 18H, [(CH₃)₂Si−]), 0.48 (t, *J* = 7.2 Hz, 2H, ZrCH₂CH₂CH₂CH₃), 0.49 (t, *J* = 7.2 Hz, 3H, ZrCH₂CH₂CH₂CH₃), 0.68 (m, 2H, ZrCH₂CH₂CH₂CH₃), 0.89 (m, 2H, ZrCH₂CH₂CH₂CH₃), 6.80–6.88 (m, 12H, [*p*-C₆H₄F]). ¹³C{¹H} NMR (20 °C, C₆D₆): δ 2.9 (s, HC≡), 3.9 ([[(CH₃)₂Si−]), 13.8 (ZrCH₂CH₂CH₂CH₃), 27.0 (ZrCH₂CH₂CH₂CH₃), 28.1 (ZrCH₂CH₂CH₂CH₃), 70.8 (s) (ZrCH₂CH₂CH₂CH₃), 116.6 (d, ²*J*_{FC} = 21.6 Hz, *meta* [*p*-C₆H₄F]), 126.1 (d, ³*J*_{FC} = 15.3 Hz, *ortho* [*p*-C₆H₄F]), 143.3 (*ipso* [*p*-C₆H₄F]), 158.8 (d, ¹*J*_{FC} = 239, *para* [*p*-C₆H₄F]).

General procedure for catalytic hydrosilations

A reaction flask with a Teflon valve was charged with catalyst (0.08 mmol), PhSiH₃ (4.00 mmol), and olefin (4.00 mmol) in the glove box. No solvent was added. The flask was sealed and placed in a 90 °C oil bath. Small aliquots of the reaction mixture were withdrawn periodically, and their ¹H NMR spectra were taken to monitor the progress of the reaction. When the reaction was completed, the product was separated

from the catalyst by distillation under reduced pressure. The NMR spectra of the products are compared to the data reported in the literature.^{15,16}

X-Ray structure determination

Crystals of **1b**, **2a**, **3a**, and **3b** were placed on the tip of a 0.1 mm diameter glass capillary and mounted on a Siemens or Bruker SMART Platform CCD diffractometer for data collection at 173(2) K using graphite-monochromated Mo-K α radiation (0.71703 Å). The intensity data were corrected for Lorentz polarization effects, absorption, and decay.^{19,20} Final cell constants were calculated from the *xyz* centroids of 3377, 3883, 3495, and 4085 strong reflections for structures **1b**, **2a**, **3a**, and **3b**, respectively. Data are summarised in Table 6.

The structures were solved by direct methods using SIR92²¹ for **1b** and **2a** and using SHELXS-97²² for **3a** and **3b**, which provided most non-hydrogen atoms. The space groups were determined based on systematic absences and intensity statistics. Full-matrix least squares/difference Fourier cycles were performed using SHELXL-97,²³ which located the remaining non-hydrogen atoms. All non-hydrogen atoms were refined with anisotropic displacement parameters. All hydrogen atoms were placed in ideal positions and refined as riding atoms with isotropic displacement parameters related to the parent atom.

One side of the dimeric **2a** is disordered over two positions (77 : 23). Some variances in the Zr–N distances are present in the minor component of the disorder (Zr1–N1', Zr1–N2', Zr1–N3'), due to the particular modeling of the disorder. The butyl group of **3a** is modeled as disordered over two positions (50 : 50), and methyl group C21 is rotationally disordered. All the methyl groups attached to silicon atoms in **3b** are rotationally disordered.

CCDC reference numbers 183853–183856.

See <http://www.rsc.org/suppdata/dt/b2/b200789d/> for crystallographic data in CIF or other electronic format.

Acknowledgements

This work is supported by ACS-Petroleum Research Fund (Grant number 35538–G3) and Lehigh University.

References and notes

- Reviews of cationic metallocenes and olefin polymerization: (a) A thematic issue on olefin polymerization: *Chem. Rev.*, 2000, **vol. 100**; (b) H. C. L. Abbenhuis, *Angew. Chem., Int. Ed.*, 1999, **38**, 1058; (c) A. L. McKnight and R. M. Waymouth, *Chem. Rev.*, 1998, **98**, 2587; (d) W. Kaminsky, *J. Chem. Soc., Dalton Trans.*, 1998, 1413; (e) A. A. Montagna, A. H. Dekmezian and R. M. Burkhardt, *CHEMTECH*, 1997, **27**, 26; (f) M. Bochmann, *J. Chem. Soc., Dalton Trans.*, 1996, 255; (g) H. H. Brintzinger, D. Fischer, R. Mülhaupt, B. Rieger and R. M. Waymouth, *Angew. Chem., Int. Ed. Engl.*, 1995, **34**, 1143; (h) T. J. Marks, *Acc. Chem. Res.*, 1992, **25**, 57; (i) R. F. Jordan, *Adv. Organomet. Chem.*, 1991, **32**, 325.
- Cationic olefin polymerization catalysts containing amide ligands: (a) Y. Schrodi, R. R. Schrock and P. J. Bonitatebus, Jr., *Organometallics*, 2001, **20**, 3560 and references therein; (b) F. Guerin, D. H. McConville, J. J. Vittal and G. A. P. Yap, *Organometallics*, 1998, **17**, 5172 and references therein; (c) J. M. Wright, C. R. Landis, M. A. M. P. Ros and A. D. Horton, *Organometallics*, 1998, **17**, 5031 and references therein.
- (a) G. Pindado Jimenez, S. J. Lancaster, M. Thornton-Pet and M. Bochmann, *J. Am. Chem. Soc.*, 1998, **120**, 6816; (b) A. Pastor, A. F. Kiely, L. M. Henling, M. W. Day and J. E. Bercaw, *J. Organomet. Chem.*, 1997, **528**, 65; (c) M. Yoshida, D. J. Crowther and R. F. Jordan, *Organometallics*, 1997, **16**, 1349; (d) C. Kreuder, R. F. Jordan and H. Zhang, *Organometallics*, 1995, **14**, 2993; (e) D. J. Crowther and R. F. Jordan, *Makromol. Chem., Macromol. Symp.*, 1993, **66**, 121.
- Neutral d² Group 4 compounds active for ethylene oligomerization: D. Hessen and H. van der Heijden, *J. Am. Chem. Soc.*, 1996, **118**, 11670.
- (a) R. Duchateau, H. C. L. Abbenhuis, R. A. van Santen, A. Meetsma, S. K. H. Thiele and M. F. H. van Tol, *Organometallics*, 1998, **17**, 5663. Note the zirconium and hafnium complexes are active ethylene polymerization catalysts but are zwitterionic dimers, not neutral complexes; (b) J. L. Bennett and P. T. Wolczanski, *J. Am. Chem. Soc.*, 1997, **119**, 10696; (c) C. P. Schaller, C. Cummins and P. T. Wolczanski, *J. Am. Chem. Soc.*, 1996, **118**, 591; (d) C. Cummins, G. D. Van Duyne, C. P. Schaller and P. T. Wolczanski, *Organometallics*, 1991, **10**, 164; (e) R. W. Chestnut, L. D. Durfee, P. E. Fanwick, I. P. Rothwell, K. Folting and J. C. Huffman, *Polyhedron*, 1987, **6**, 2026; (f) T. V. Lubben, P. T. Wolczanski and G. D. Van Duyne, *Organometallics*, 1984, **3**, 977; (g) R. A. Andersen, *Inorg. Chem.*, 1979, **18**, 1724.
- (a) F. Lefebvre, A. De Mallmann and J.-M. Basset, *Eur. J. Inorg. Chem.*, 1999, **3**, 361; (b) V. Dufaud and J.-M. Basset, *Angew. Chem., Int. Ed.*, 1998, **37**, 806; (c) J. Corker, F. Lefebvre, C. Lécuyer, V. Dufaud, F. Quignard, A. Choplin, J. Evans and J.-M. Basset, *Science*, 1996, **271**, 966; (d) F. Quignard, C. Lécuyer, A. Choplin and J.-M. Basset, *J. Chem. Soc., Dalton Trans.*, 1994, 1153.
- (a) H. W. Turner, R. A. Andersen, A. Zalkin and D. H. Templeton, *Inorg. Chem.*, 1979, **18**, 1221; (b) C. Airoidi, D. Bradley, H. Chudzynska, M. B. Hursthouse, A. Mali and P. R. Raithby, *J. Chem. Soc., Dalton Trans.*, 1980, 2010; (c) S. L. Latesky, J. Keddington, A. K. McMullen and I. P. Rothwell, *Inorg. Chem.*, 1985, **24**, 995.
- (a) L. H. Gade, P. Renner, H. Memmler, F. Fecher, C. H. Galka, M. Laubender, S. Rdojevic, M. McPartlin and J. W. Lauher, *Chem. Eur. J.*, 2001, **7**, 2563; (b) M. Lutz, M. Haukka, T. A. Pakkanen and L. H. Gade, *Organometallics*, 2001, **20**, 2631; (c) P. Renner, C. Galka, H. Memmler, U. Kauper and L. H. Gade, *J. Organomet. Chem.*, 1999, **591**, 71; (d) A. Schneider, L. H. Gade, M. Breuning, G. Bringmann, I. J. Scowen and M. McPartlin, *Organometallics*, 1998, **17**, 1643; (e) H. Memmler, U. Kauper, L. H. Gade, I. J. Scowen and M. McPartlin, *Chem. Commun.*, 1996, 1751; (f) B. Findeis, M. Schubart, C. Platzek, L. H. Gade, I. J. Scowen and M. McPartlin, *Chem. Commun.*, 1996, 219; (g) H. Memmler, W. Kevin, L. H. Gade and J. W. Lauher, *Inorg. Chem.*, 1995, **34**, 4062; (h) M. Schubart, B. Findeis, L. H. Gade, W.-S. Li and M. McPartlin, *Chem. Ber.*, 1995, **128**, 329; (i) S. Friedrich, H. Memmler, L. H. Gade, W.-S. Li and M. McPartlin, *Angew. Chem., Int. Ed. Engl.*, 1994, **33**, 676; (j) L. H. Gade, C. Becker and J. W. Lauher, *Inorg. Chem.*, 1993, **32**, 2308.
- L. Jia, E. Ding, A. L. Rheingold and B. Rhatigan, *Organometallics*, 2000, **19**, 963.
- S. L. Latesky, A. K. McMullen, G. P. Niccolai and I. P. Rothwell, *Organometallics*, 1985, **4**, 902.
- M. Brookhart, M. L. H. Green and L. Wong, *Prog. Inorg. Chem.*, 1988, **36**, 1.
- Z. Dawoodi, M. L. H. Green, V. S. B. Mtetwa, K. Prout, A. J. Schultz, J. M. Williams and T. F. Koetzle, *J. Chem. Soc., Dalton Trans.*, 1986, 1629.
- M. E. Thompson, S. M. Baxter, A. R. Bulls, B. J. Burger, M. C. Nolan, B. D. Santarsiero, W. P. Schaefer and J. E. Bercaw, *J. Am. Chem. Soc.*, 1987, **109**, 203–219.
- R. F. Jordan, P. K. Bradley, N. C. Baenziger and R. E. LaPointe, *J. Am. Chem. Soc.*, 1990, **112**, 1289.
- (a) G. A. Molander and M. H. Schmitt, *J. Org. Chem.*, 2000, **65**, 3767 and references therein; (b) T. I. Gountchev and T. D. Tilley, *Organometallics*, 1999, **18**, 5661; (c) P.-F. Fu, L. Brard, Y. Li and T. J. Marks, *J. Am. Chem. Soc.*, 1995, **117**, 7157; (d) T. Skakura, H. Lautenschlager and M. J. Tanaka, *J. Chem. Soc., Chem. Commun.*, 1991, 40.
- (a) E.-I. Negishi and T. Takahashi, *Acc. Chem. Res.*, 1994, **27**, 124; (b) J. Y. Corey and X.-H. Zhu, *Organometallics*, 1992, **11**, 672; (c) T. Takahashi, M. Hasegawa, N. Suzuki, M. Souri, C. J. Rousset, P. E. Fanwick and E.-I. Negishi, *J. Am. Chem. Soc.*, 1990, **112**, 1291.
- (a) D. Churchill, J. H. Shin, T. Hascall, J. M. Hahn, B. M. Bridgewater and G. Parkin, *Organometallics*, 1999, **18**, 2404; (b) J. H. Shin and G. Parkin, *Chem. Commun.*, 1999, 887; (c) H. Lee, P. J. Desrosiers, I. Guzei, A. Rheingold and G. Parkin, *J. Am. Chem. Soc.*, 1998, **120**, 3255.
- U. Zucchini, E. Albizzati and U. Giannini, *J. Organomet. Chem.*, 1971, **260**, 357.
- An empirical correction for absorption anisotropy: R. Blessing, *Acta Crystallogr., Sect. A*, 1995, **51**, 33.
- SAINT version 6.1, Bruker Analytical Systems, Madison, WI, 1999.
- SIR92, A. Altomare, C.ascarano, C. Giacovazzo and A. Gualardi, *J. Appl. Crystallogr.*, 1993, **26**, 343.
- G. M. Sheldrick, Program for Crystal Structure Solution, Universität Göttingen, Göttingen, 1997.
- G. M. Sheldrick, Program for Crystal Structure Refinement, Universität Göttingen, Göttingen, 1997.
- M. N. Burnett and C. K. Johnson, ORTEP3, Report ORNL-6895, Oak Ridge National Laboratory, Oak Ridge, TN, 1996.